Cosmological shocks and magnetic fields in galaxy clusters

Christoph Pfrommer[1]

in collaboration with

Jonathan Dursi[2], Tom Jones[3]

[1]Heidelberg Institute for Theoretical Studies, Germany
[2]Canadian Institute for Theoretical Astrophysics/SciNet Consortium, Canada
[3]University of Minnesota, Department of Astronomy, Minneapolis, USA

Apr 28, 2011 / Stanford Astrophysics Colloquium

Outline

Outline

The structure of our Universe

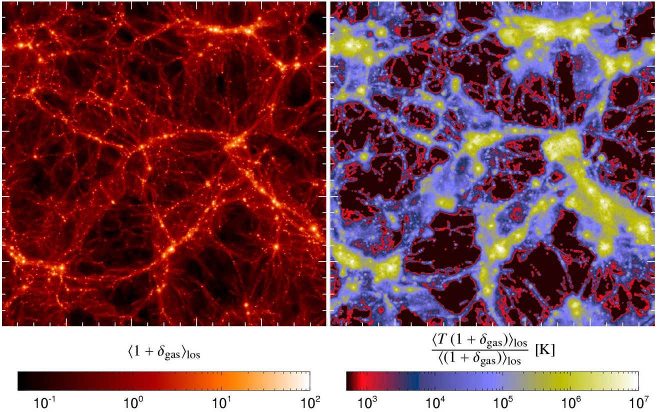

The "cosmic web" today. *Left:* the projected gas density in a cosmological simulation. *Right:* gravitationally heated intracluster medium through cosmological shock waves (C.P. et al. 2006).

A theorist's perspective of a galaxy cluster . . .

Galaxy clusters are dynamically evolving dark matter potential wells:

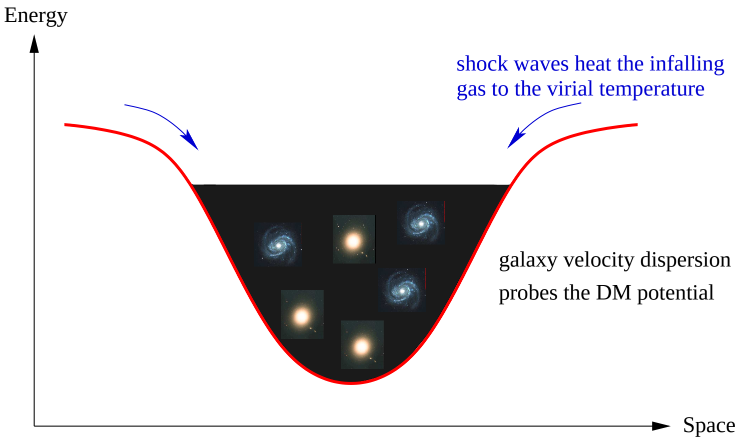

. . . and how the observer's Universe looks like

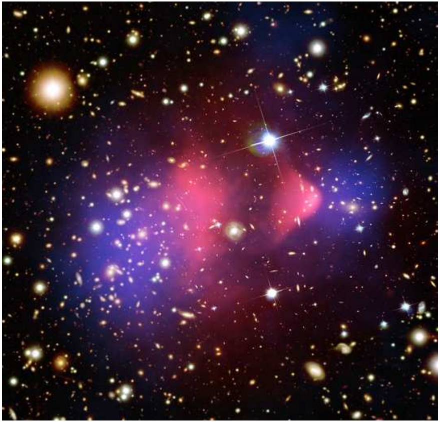

1E 0657-56 ("Bullet cluster")

(X-ray: NASA/CXC/CfA/M.Markevitch et al.; Optical: NASA/STScI; Magellan/U.Arizona/D.Clowe et al.; Lensing: NASA/STScI; ESO WFI; Magellan/U.Arizona/D.Clowe et al.)

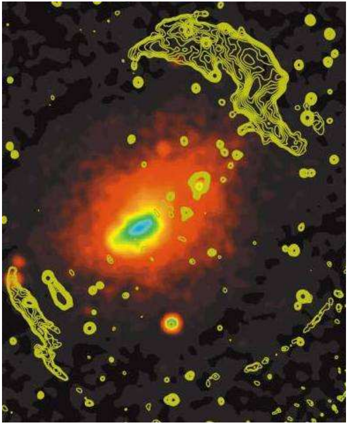

Abell 3667

(radio: Johnston-Hollitt. X-ray: ROSAT/PSPC.)

Wish list for shocks

What we would like to measure and hope to infer:

- jump conditions: shock strength
- upstream properties: infalling warm-hot intergalactic medium
- post- and pre-shock conditions: geometry, obliquity
- shock curvature: vorticity and B field generation
- post-shock turbulence: power spectrum, non-thermal pressure support
- ...

X-rays give limited insight → new complementary tools!

Wish list for shocks

What we would like to measure and hope to infer:

- jump conditions: shock strength
- upstream properties: infalling warm-hot intergalactic medium
- post- and pre-shock conditions: geometry, obliquity
- shock curvature: vorticity and B field generation
- post-shock turbulence: power spectrum, non-thermal pressure support
- ...

X-rays give limited insight → new complementary tools!

Total synchrotron intensity of NGC 1265

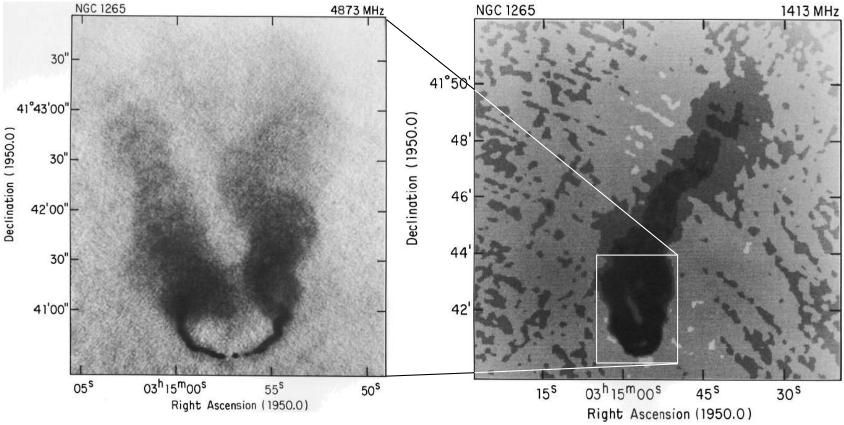

O'Dea & Owen (1986): 4.9 GHz *(left)* and 1.4 GHz *(right)*

Bipolar AGN jets in an ICM wind: magnetic field

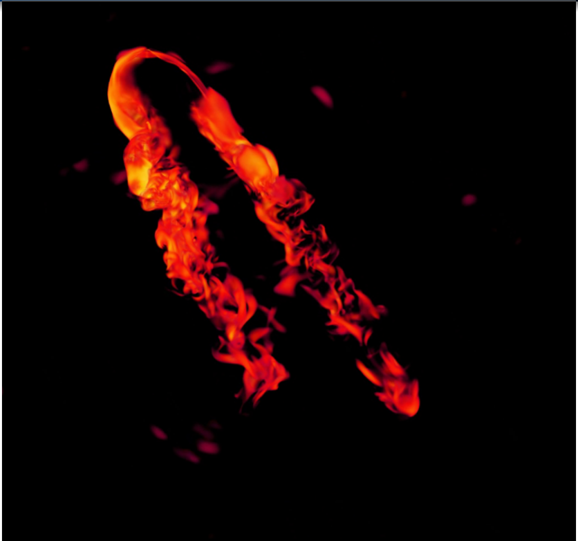

credit: Porter, Mendygral & Jones

Bipolar AGN jets in an ICM wind: synthetic radio

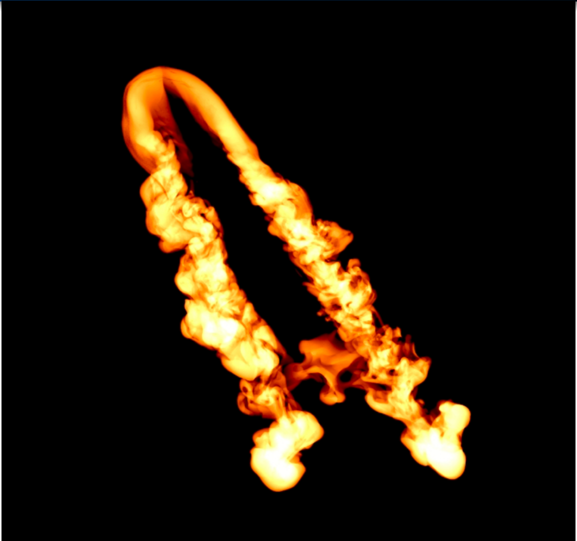

credit: Porter, Mendygral & Jones

Radio properties of NGC 1265

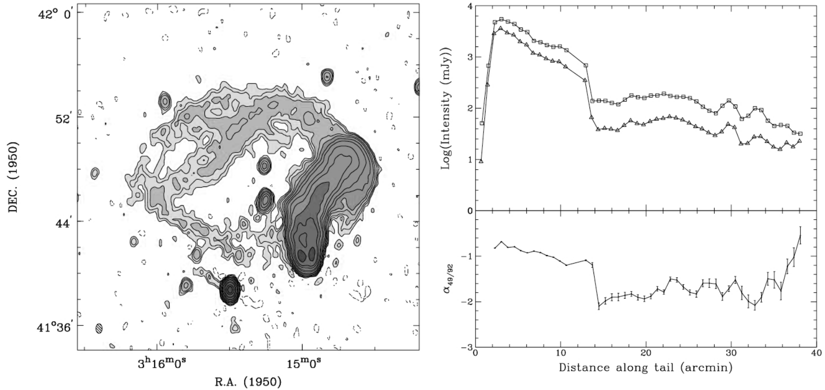

Sijbring & de Bruyn (1998), *left:* radio intensity $I_{600\,\mathrm{MHz}}$; *right:* variations of $I_{600\,\mathrm{MHz}}$ *(triangles)*, $I_{150\,\mathrm{MHz}}$ *(squares)* and spectral index *(bottom)* along the tail

Previous models of NGC 1265 and why they fail

1. chance superposition of several independent head-tail galaxies
   $\rightarrow$ *lack of observed strong radio sources in this field*

Previous models of NGC 1265 and why they fail

1. chance superposition of several independent head-tail galaxies
   $\rightarrow$ *lack of observed strong radio sources in this field*
2. re-acceleration of electrons in the turbulent wake of a galaxy
   $\rightarrow$ *contrived projection probabilities and implausible energetics (re-acceleration efficiency* $\sim 3\%$*)*

Previous models of NGC 1265 and why they fail

1. chance superposition of several independent head-tail galaxies
   → *lack of observed strong radio sources in this field*
2. re-acceleration of electrons in the turbulent wake of a galaxy
   → *contrived projection probabilities and implausible energetics (re-acceleration efficiency* $\sim 3\%$*)*
3. ‘radio tail’ traces a helical cluster wind
   → *wind needs special alignment with LOS, fine-tuned re-acceleration that balances electron cooling and avoids fanning out the well-confined radio emission along the arc*

Previous models of NGC 1265 and why they fail

1. chance superposition of several independent head-tail galaxies
   $\rightarrow$ *lack of observed strong radio sources in this field*
2. re-acceleration of electrons in the turbulent wake of a galaxy
   $\rightarrow$ *contrived projection probabilities and implausible energetics (re-acceleration efficiency* $\sim 3\%$*)*
3. 'radio tail' traces a helical cluster wind
   $\rightarrow$ *wind needs special alignment with LOS, fine-tuned re-acceleration that balances electron cooling and avoids fanning out the well-confined radio emission along the arc*
4. 'radio tail' outlines ballistic orbit of NGC 1265
   $\rightarrow$ *requires dark object with* $M \gtrsim M_{\mathrm{NGC\ 1265}} \simeq 3 \times 10^{12} M_{\odot}$ *orbiting the galaxy, no explanation of change of orbit and same challenges regarding electron cooling and re-acceleration*

Requirements for any model of NGC 1265

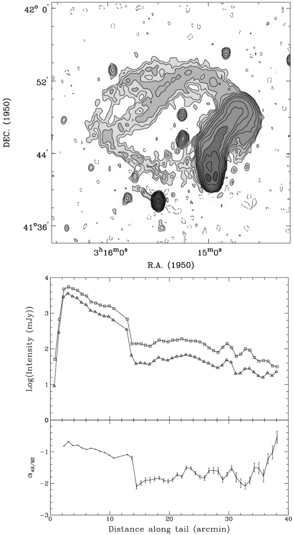

- bright narrow angle tail radio jet: synchrotron cooling
- transition region: change of winding direction and sharp drop in S_ν and α
- coherent properties along the dim radio ring, confined morphology

$\rightarrow$ *we are looking at 2 electron populations in projection possibly suggesting 2 different epochs of feedback:*

$\rightarrow$ active jet + detached radio bubble that recently got energized coherently across 300 kpc $\rightarrow$ shock?

Shock overruns an aged radio bubble (C.P. & Jones 2011)

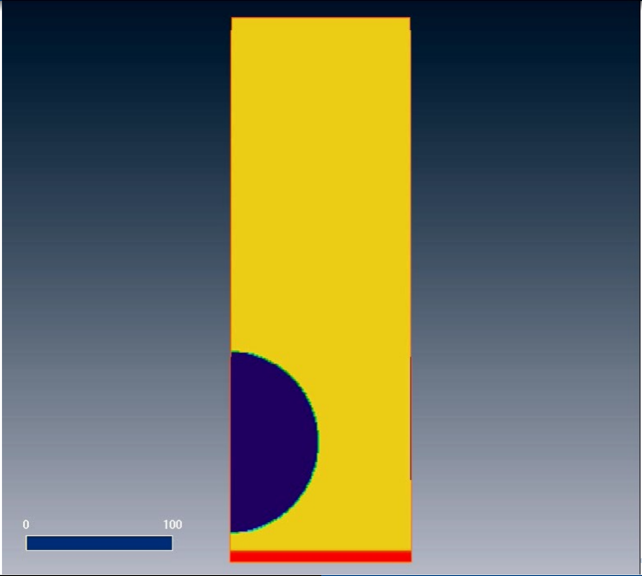

Bubble transformation to vortex ring

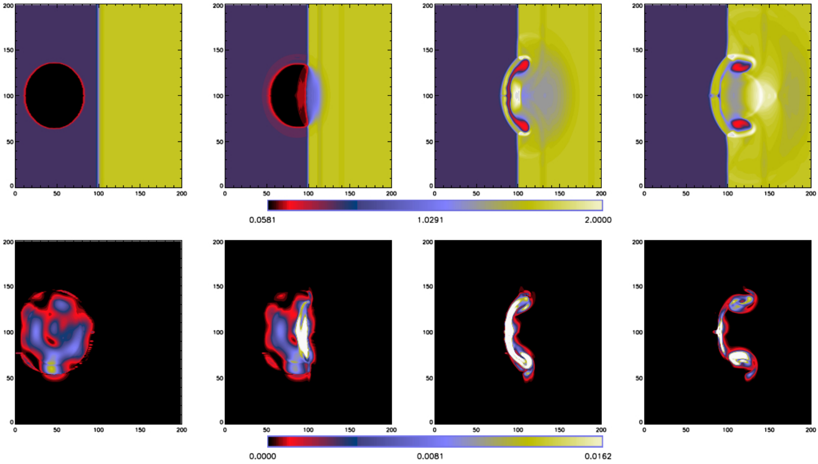

Enßlin & Brüggen (2002): gas density *(top)* and magnetic energy density *(bottom)*

Synthetic radio emission of shock-transformed bubble

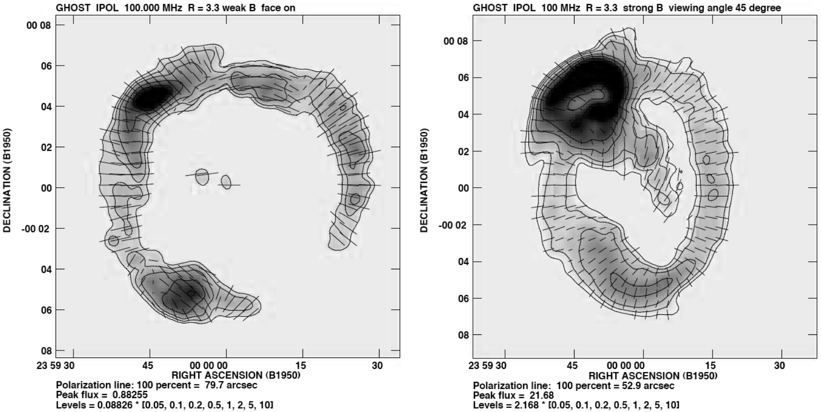

Enßlin & Brüggen (2002): total 100 MHz intensity and polarization E-vectors, strong shock/weak *B (left)* and strong shock/strong *B* model *(right)*

HITS

Cartoon of the time evolution of NGC 1265

C.P. & Jones (2011):

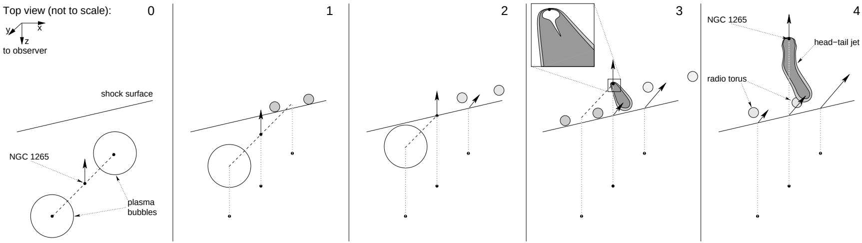

NGC 1265 as a perfect probe of a shock

- **idea:**
  - galaxy velocity not affected by shock
    $\longrightarrow$ pre-shock conditions
  - tail & torus as tracers of the post-shock flow
- **assumptions:**
  - shock surface $\parallel$ gravitational equipotential surface of Perseus
  - recent jet launched shortly after shock crossing
- **method:**
  - extrapolating position and velocity back in time
  - employing conservation laws at oblique shock
  - iterate until convergence

Derived geometry for NGC 1265

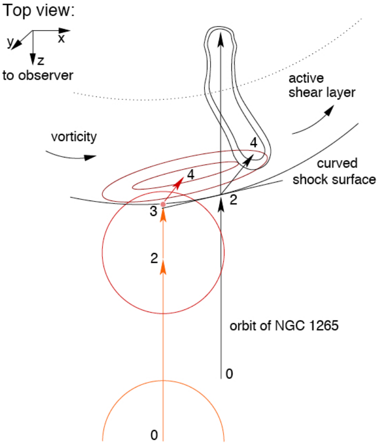

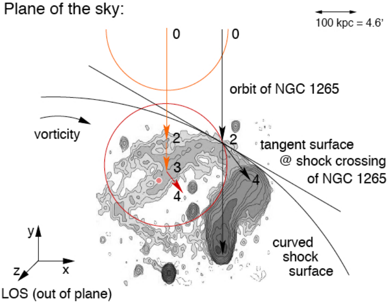

C.P. & Jones (2011)

Shock strength and jump conditions

- shock compresses relativistic bubble adiabatically: $P_2/P_1 = C^{4/3}$
- bubble compression factor:

$$C = \frac{V_{\rm bubble}}{V_{\rm torus}} = \frac{\frac{4}{3}\pi R^3}{2\pi^2 R r_{\rm min}^2} = \frac{2}{3\pi}\left(\frac{R}{r_{\rm min}}\right)^2 \simeq 10$$

- assuming pressure equilibrium → shock jumps:

$$\frac{P_2}{P_1} \simeq 21.5, \quad \frac{\rho_2}{\rho_1} \simeq 3.4, \quad \frac{T_2}{T_1} \simeq 6.3, \quad \text{and } \mathcal{M} \simeq 4.2$$

C.P. & Jones (2011)

Perseus accretion shock and WHIM properties

- jet has low Faraday RM → NGC 1265 on near side of Perseus
  NGC 1265 redshifted w/r to Perseus → infalling system
  → shock likely the accretion shock
- extrapolating X-ray n- and T-profiles to R_{200} & shock jumps:
  → upper limits on infalling warm-hot intergalactic medium

$$
\begin{aligned}
kT_1 &\lesssim 0.4\,\mathrm{keV} \\
n_1 &\lesssim 5\times10^{-5}\,\mathrm{cm}^{-3} \\
P_1 &\lesssim 3.6\times10^{-14}\,\mathrm{erg\,cm}^{-3}
\end{aligned}
$$

C.P. & Jones (2011)

Shear flows and shock curvature

- ellipticity of radio torus (magnitude and orientation) & bending direction of tail
  $\rightarrow$ excludes projection effects
  $\rightarrow$ evidence for post-shock shear flow
- shock curvature injects vorticity that shears the gas westwards:

$$\frac{\varepsilon_{\mathrm{shear}}}{\varepsilon_{\mathrm{th},2}} = \frac{\mu m_{\mathrm{p}} v_\perp^2}{3kT_2} \simeq 0.14,$$

with $kT_2 \simeq 2.4\,\mathrm{keV}$ and $v_\perp \simeq 400\,\mathrm{km/s}$.

C.P. & Jones (2011)

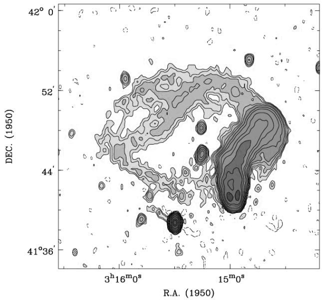

Sijbring & de Bruyn (1998)

Conclusions on radio galaxies as probes of shocks

- consistent 3D model of NGC 1265
- prediction of a very interesting source class for LOFAR
- radio galaxies as perfect probes of pre- and post-shock flows:
  - hydrodynamic jumps and Mach numbers
  - statistical properties of the infalling WHIM (+ X-rays)
  - estimating the curvature radius of shocks and induced shear flows

→ implications for intra-cluster turbulence as well as generation and amplification of large-scale magnetic fields!

Outline

What is magnetic draping?

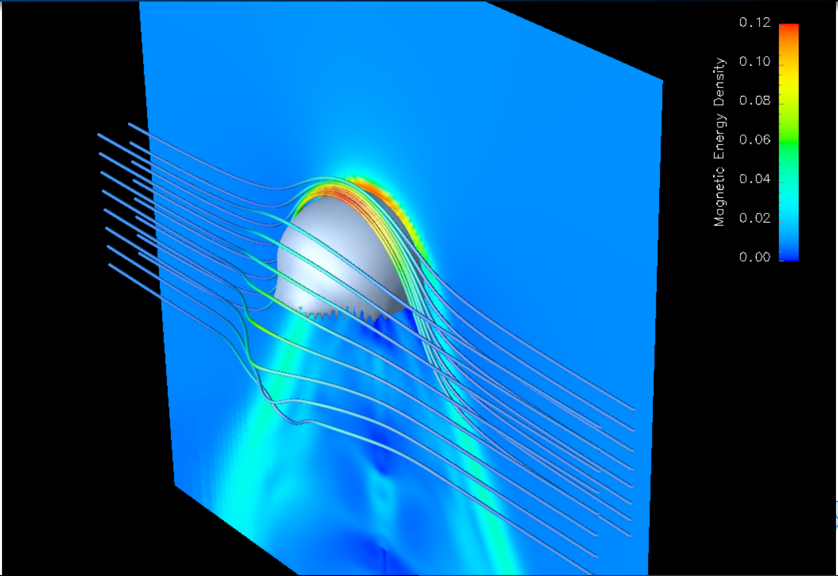

What is magnetic draping?

- Is magnetic draping (MD) similar to ram pressure compression?
  $\longrightarrow$ no density enhancement for MD
  - analytical solution of MD for incompressible flow
  - ideal MHD simulations *(right)*
- Is magnetic flux still frozen into the plasma?
  yes, but plasma can also move along field lines while field lines get stuck at obstacle

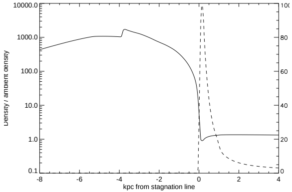

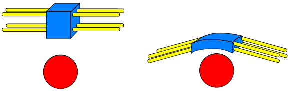

Applications of magnetic draping

- solar system: plasma physics
- hydrodynamic stability of radio bubbles
  (Dursi 2007, Ruszkowski+2007)
- sharpness (T_e, n_e) of cold fronts: without B, smoothed out by diffusion and heat conduction on $\gtrsim 10^8$ yrs
  (Lyutikov 2004, Dursi+2008)

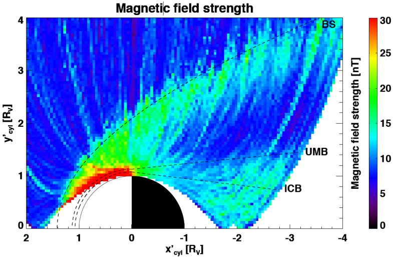

Guicking et al. (2010): magnetic draping around Venus

- magnetic draping on spiral galaxies: method for detecting the orientation of cluster fields (C.P.+2010)

Magnetic draping in 2D

Sometimes,
2D just isn't
enough ...

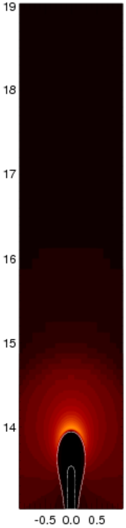

MHD solution: kinematic approx. vs. AMR simulation

B_x, B_y, B_z in the plane of the initial B-field

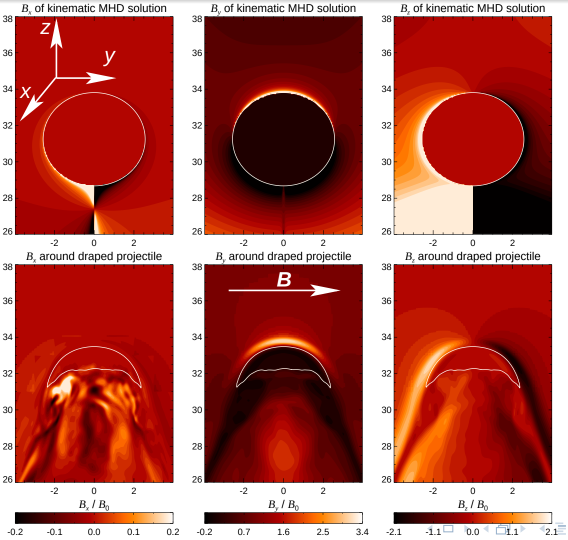

MHD solution: kinematic approx. vs. AMR simulation

B_x, B_y, B_z in the plane perpendicular to the initial B-field

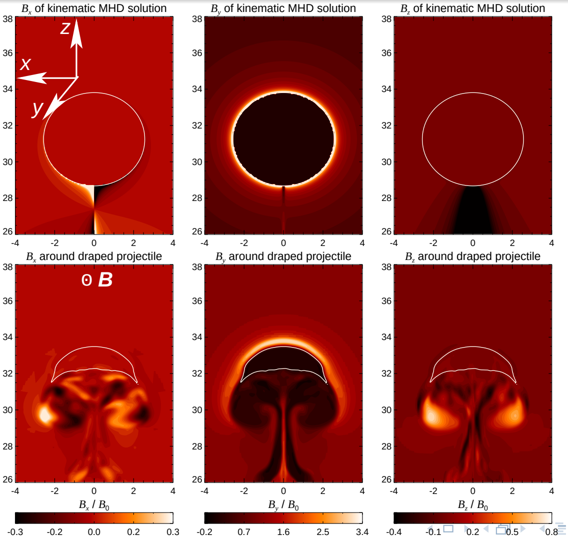

Thickness of the draping sheath – simulations

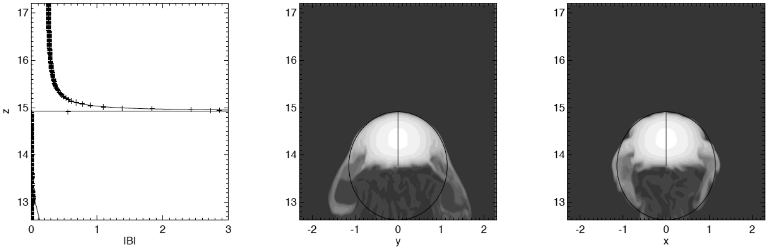

amplified draping field $B = \frac{B_0}{\sqrt{1-\frac{R^3}{r^3}}}$, $\quad l_{\rm drape} \simeq \frac{R}{12\mathcal{M}_{\rm A}^2} \simeq (10 - 100)$ pc

left: fitting peak position and a fall-off radius of the theory prediction; *right:* density cut-planes; circle shows radius and position given by the fit to the magnetic field structure, left;

→ astonishing agreement of curvature radius at the working surface with potential flow predictions!

Streamlines in the rest frame of the galaxy

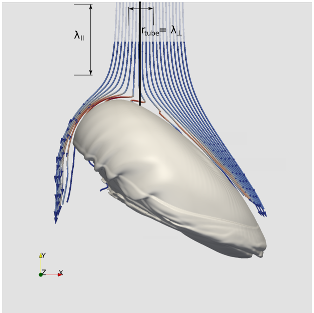

- Stokes function $p(s, \theta) = \sqrt{3sR}\,\sin\theta$ $\rightarrow$ critical impact parameter for $\theta = \pi/2$, $s = l_{\rm drape}$: $p_{\rm cr} = R/(2\mathcal{M}_A)$
- only those streamlines initially in a narrow tube of radius $p_{\rm cr} \simeq R/20 \simeq 1$ kpc from the stagnation line become part of the magnetic draping layer (color coded) $\rightarrow$ constraints on λ_B
- the streamlines that do not intersect the tube get deflected away from the galaxy, become never part of the drape and eventually get accelerated (Bernoulli effect)
- note the kink feature in some draping-layer field lines due to back reaction as the solution changes from the hydrodynamic potential flow solution to that in the draped layer

Streamlines in the rest frame of the galaxy

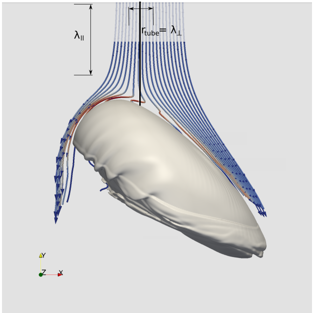

- Stokes function $p(s,\theta) = \sqrt{3sR}\,\sin\theta$ $\rightarrow$ critical impact parameter for $\theta = \pi/2$, $s = l_{\rm drape}$: $p_{\rm cr} = R/(2\mathcal{M}_A)$
- only those streamlines initially in a narrow tube of radius $p_{\rm cr} \simeq R/20 \simeq 1$ kpc from the stagnation line become part of the magnetic draping layer (color coded) $\rightarrow$ constraints on λ_B
- the streamlines that do not intersect the tube get deflected away from the galaxy, become never part of the drape and eventually get accelerated (Bernoulli effect)
- note the kink feature in some draping-layer field lines due to back reaction as the solution changes from the hydrodynamic potential flow solution to that in the draped layer

Conditions for magnetic draping

- ambient plasma sufficiently ionized such that flux freezing condition applies
- super-Alfvénic motion of a cloud through a weakly magnetized plasma: $\mathcal{M}_A^2 = \beta\gamma\mathcal{M}^2/2 > 1$
- magnetic coherence across the "cylinder of influence":

$$\frac{\lambda_B}{R} \gtrsim \frac{1}{\mathcal{M}_A} \sim 0.1 \times \left(\frac{\beta}{100}\right)^{-1/2} \quad \text{for sonic motions,}$$

Here R denotes the curvature radius of the working surface at the stagnation line.

Outline

Polarized synchrotron emission in a field spiral: M51

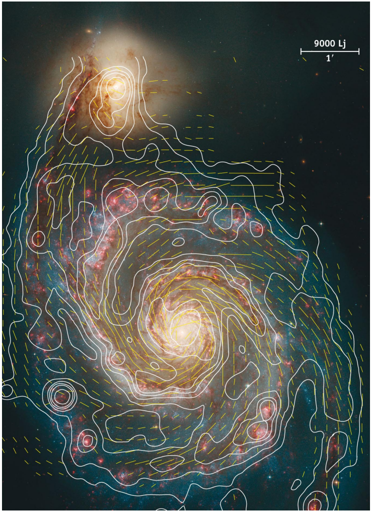

MPIfR Bonn and Hubble Heritage Team

- grand design ‘whirlpool galaxy’ (M51): optical star light superposed on radio contours
- polarized radio intensity follows the spiral pattern and is strongest in between the spiral arms
- the polarization ‘B-vectors’ are aligned with the spiral structure

Ram-pressure stripping of cluster spirals

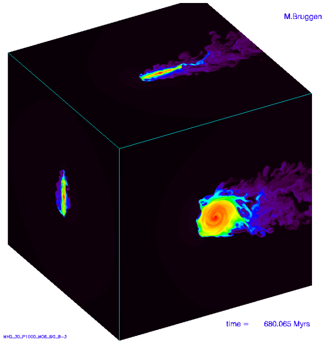

Brueggen (2008)

- 3D simulations show that the ram-pressure wind quickly strips the low-density gas in between spiral arms (Tonnesen & Bryan 2010)
- being flux-frozen into this dilute plasma, the large scale magnetic field will also be stripped

$\rightarrow$ resulting radio emission should be unpolarized

Polarized synchrotron ridges in Virgo spirals

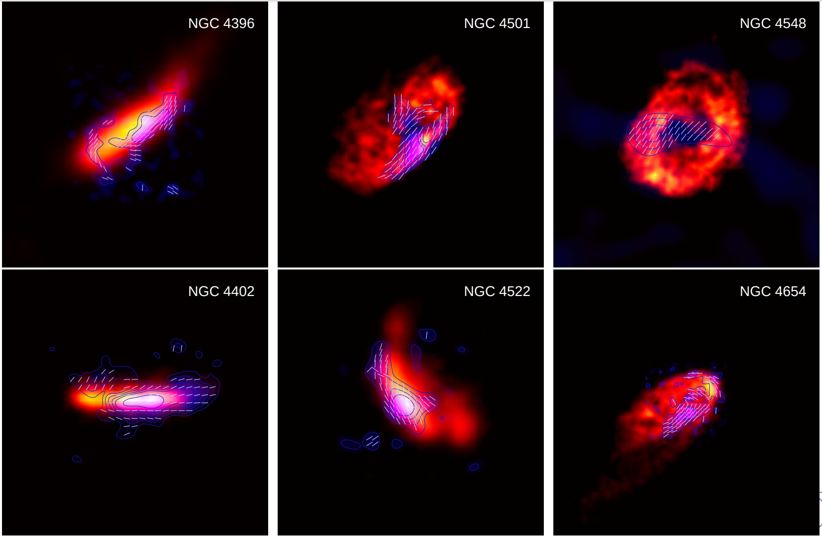

Vollmer et al. (2007): 6 cm PI (contours) + B-vectors; Chung et al. (2009): HI (red)

Magnetic draping around a spiral galaxy

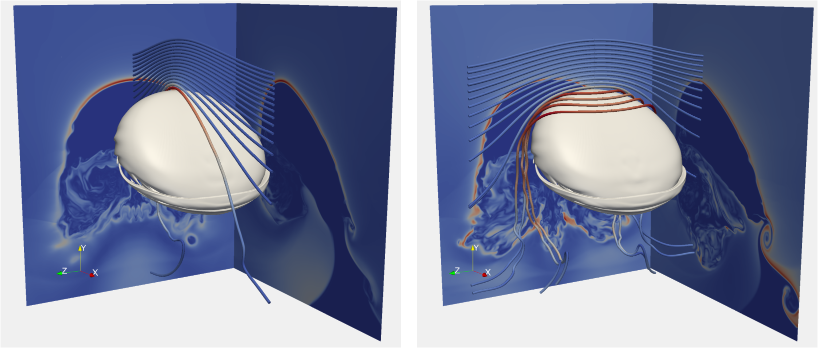

Athena simulations of spiral galaxies interacting with a uniform cluster magnetic field. There is a sheath of strong field draped around the leading edge (shown in red). C.P. & Dursi, 2010, Nature Phys.

Magnetic draping around a spiral galaxy – physics

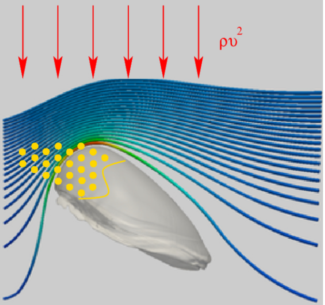

- the galactic ISM is pushed back by the ram pressure wind $\sim \rho \upsilon^2$
- the stars are largely unaffected and lead the gas
- the draping sheath is formed at the contact of galaxy/cluster wind
- as stars become SN, their remnants accelerate CRes that populate the field lines in the draping layer

- CRes are transported diffusively (along field lines) and advectively as field lines slip over the galaxy
- CRes emit radio synchrotron radiation in the draped region, tracing out the field lines there $\rightarrow$ coherent polarized emission at the galaxies' leading edges

Modeling the electron population

- cooling time scale of synchrotron emitting electrons (CRe):

$$\nu_{\rm sync} = \frac{3eB}{2\pi\, m_{\rm e} c}\,\gamma^2 \simeq 5\ {\rm GHz}\left(\frac{B}{7\,\mu{\rm G}}\right)\left(\frac{\gamma}{10^4}\right)^2,$$

$$\tau_{\rm sync} = \frac{E}{\dot{E}} = \frac{6\pi m_{\rm e} c}{\sigma_{\rm T} B^2 \gamma} = 5\times 10^7\ {\rm yr}\left(\frac{\gamma}{10^4}\right)^{-1}\left(\frac{B}{7\,\mu{\rm G}}\right)^{-2}$$

- typical SN rates imply a homogeneous CRe distribution (WMAP)
- FIR-radio correlation of Virgo spirals show comparable values to the solar circle: take MW CRe distribution inside our galaxies,

$$n_{\rm cre} = C_0\, e^{-(R-R_\odot)/h_R}\, e^{-|z|/h_z}$$

with normalization $C_0 \simeq 10^{-4}\,{\rm cm}^{-3}$ as well as scale heights $h_R \simeq 8\,{\rm kpc}$ and $h_z \simeq 1\,{\rm kpc}$, normalized at Solar position

- truncate at contact of ISM-ICM, attach exp. CRe distribution $\perp$ to contact surface with $h_\perp \simeq 150$ pc (max. radius of Sedov phase)

Magnetic draping and polarized synchrotron emission

Synchrotron B-vectors reflect the upstream orientation of cluster magnetic fields

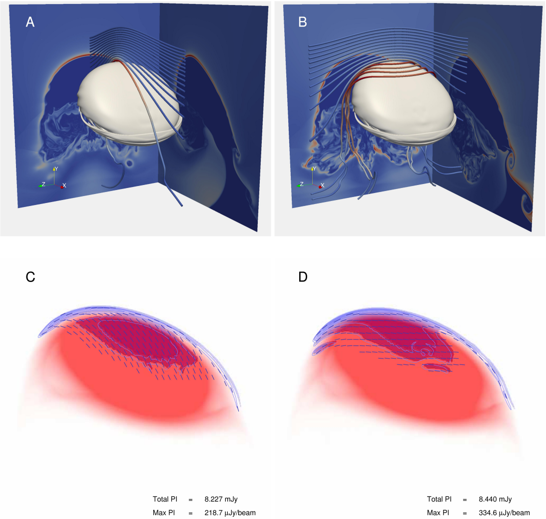

Magnetic draping of a helical B-field

(Non-)observation of polarization twist constrains magnetic coherence length

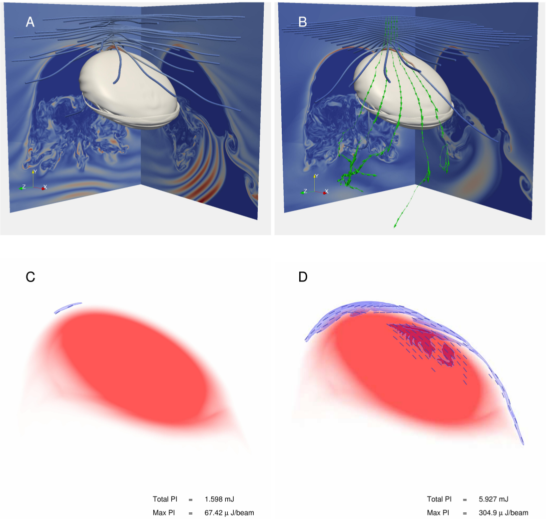

Magnetic coherence scale estimate by radio ridges

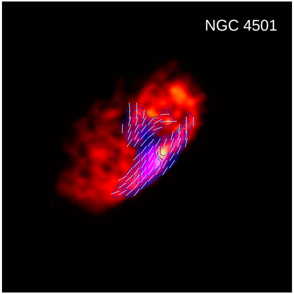

- observed polarised draping emission $\rightarrow$ field coherence length λ_B is at least galaxy-sized
- if $\lambda_B \sim 2R_{\rm gal}$, then the change of orientation of field vectors imprint as a change of the polarisation vectors along the vertical direction of the ridge showing a 'polarisation-twist'
- the reduced speed of the boundary flow means that a small $L_{\rm drape}$ corresponds to a larger length scale of the unperturbed magnetic field ahead of the galaxy NGC 4501

$$L_{\rm coh} \simeq \eta L_{\rm drape} v_{\rm gal}/v_{\rm drape} = \eta \tau_{\rm syn} v_{\rm gal} > 100\,{\rm kpc},$$

with $\tau_{\rm syn} \simeq 5 \times 10^7$ yr, $v_{\rm gal} \simeq 1000\,{\rm km/s}$, and a geometric factor $\eta \simeq 2$

Varying galaxy inclination and magnetic tilt

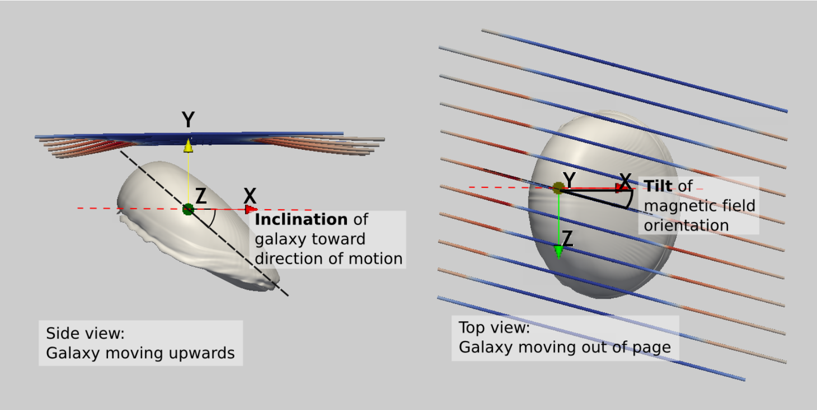

Observations versus simulations

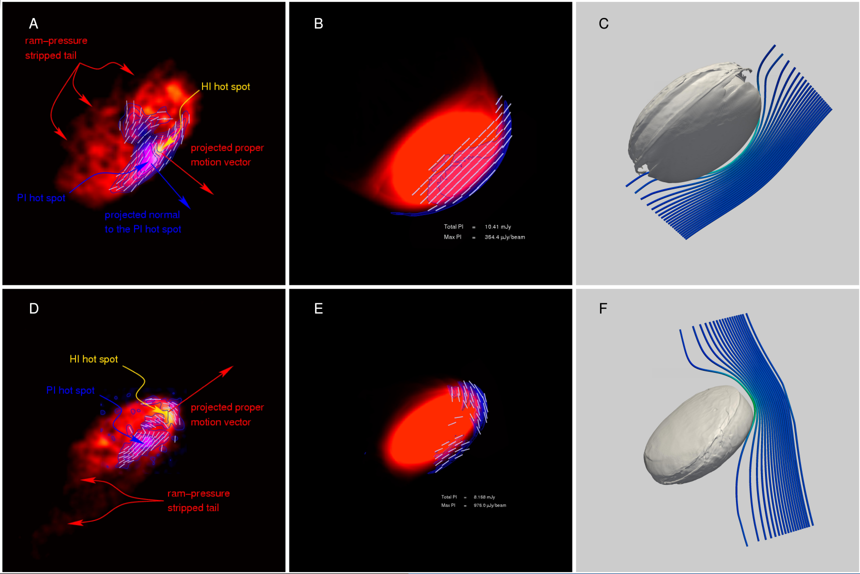

Biases in inferring the field orientation

- uncertainties in estimating the 3D velocity: v_r, ram-pressure stripped gas visible in HI morphology $\rightarrow \hat{\boldsymbol{v}}_\mathrm{t}$
- *direction-of-motion asymmetry:* magnetic field components in the direction of motion bias the location of $B_{\mathrm{max,\ drape}}$ (figure to the right): draping is absent if $\boldsymbol{B} \parallel \boldsymbol{v}_\mathrm{gal}$

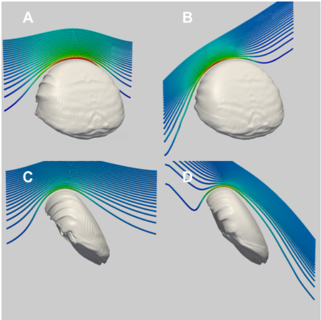

- *geometric bias:* polarized synchrotron emission only sensitive to traverse magnetic field B_t ($\perp$ to LOS) $\rightarrow$ maximum polarised intensity may bias the location of $B_{\mathrm{max,\ drape}}$ towards the location in the drape with large B_t

Mapping out the magnetic field in Virgo

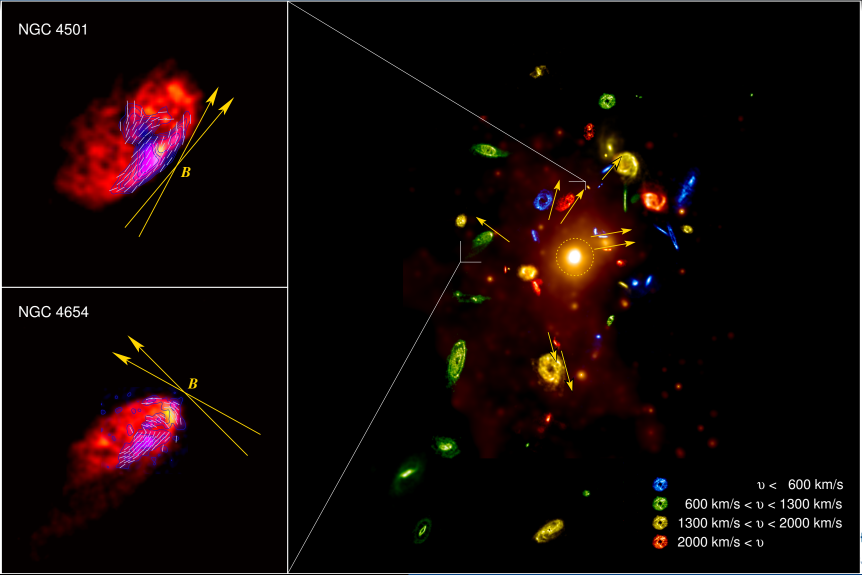

Discussion of radial field geometry

- The alignment of the field in the plane of the sky is significantly more radial than expected from random chance. Considering the sum of deviations from radial alignment gives a chance coincidence of less than 1.7% ($\sim 2.2\,\sigma$).
- For the three nearby galaxy pairs in the data set, all have very similar field orientations.

$\rightarrow$ Which effect causes this field geometry?

Radial infall? (Ruszkowski+2010)

Magneto-thermal instability? (Parrish+2007, C.P.+2010)

Magneto-thermal instability: the idea

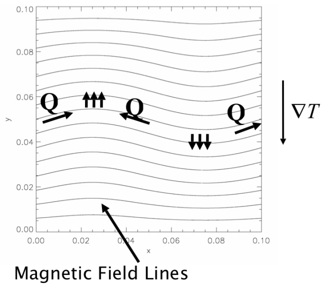

Figure from I. Parrish

Convective stability in a gravitational field:

- Classical Schwarzschild criterion: $\frac{\mathrm{d}S}{\mathrm{d}z} > 0$
- long MFP, Balbus criterion: $\frac{\mathrm{d}T}{\mathrm{d}z} > 0$
- new instability causes field lines to reorient radially $\rightarrow$ efficient thermal conduction radially

The non-linear behavior of the MTI (Parrish & Stone 2007).

- Adiabatic boundary conditions for $T(r)$: the instability can exhaust the source of free energy $\rightarrow$ isothermal profile
- Fixed boundary conditions for $T(r)$: field lines stay preferentially radially aligned (35 deg mean deviation from radial)

Magneto-thermal instability: the idea

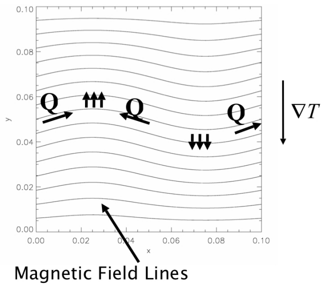

Figure from I. Parrish

Convective stability in a gravitational field:

- Classical Schwarzschild criterion: $\frac{\mathrm{d}S}{\mathrm{d}z} > 0$
- long MFP, Balbus criterion: $\frac{\mathrm{d}T}{\mathrm{d}z} > 0$
- new instability causes field lines to reorient radially $\rightarrow$ efficient thermal conduction radially

The non-linear behavior of the MTI (Parrish & Stone 2007).

- Adiabatic boundary conditions for $T(r)$: the instability can exhaust the source of free energy $\rightarrow$ isothermal profile
- Fixed boundary conditions for $T(r)$: field lines stay preferentially radially aligned (35 deg mean deviation from radial)

Gravitational shock wave heating

Observed temperature profile in clusters is decreasing outwards
→ heat also flows outwards along the radial magnetic field.
How is the temperature profile maintained? → gravitational heating

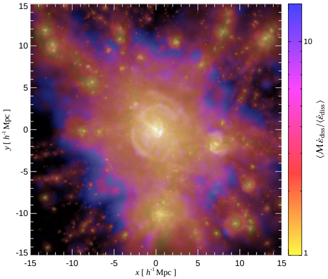

shock strengths weighted by dissipated energy

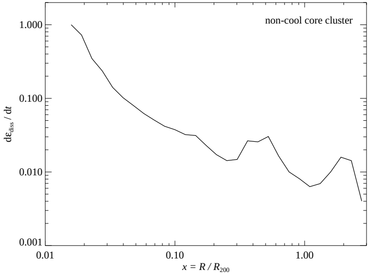

energy flux through shock surface $\dot{E}_{\mathrm{diss}} / R^2 \sim \rho \upsilon^3$
→ increase towards the center

Implications for galaxy clusters (probing cosmology)

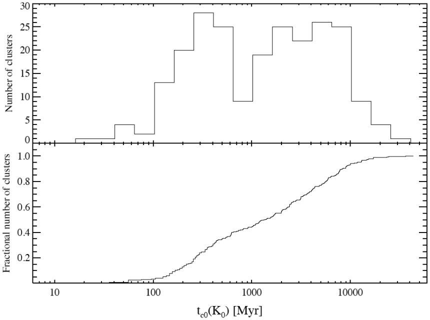

Cavagnolo et al. (2009)

- *How are galaxy clusters thermally stabilized?*
  → radial magnetic field in non-cool core clusters implies efficient thermal conduction that stabilizes these systems against entering a cooling catastrophe
  → thermal history + clusters as cosmological probes
- current cosmological cluster simulations fail to reproduce these clusters
  → magnetic fields + anisotropic conduction

Speculation: evolutionary sequence of galaxy clusters

- After a merging event of a non-cool core cluster, the injected turbulence decays on an eddy turnover time $\tau_\text{eddy} \simeq L_\text{eddy}/\upsilon_\text{turb} \sim 300\,\text{kpc}/(300\,\text{km/s}) \sim 1$ Gyr.
- The magneto-thermal instability grows on a similar timescale of less than 1 Gyr and the magnetic field becomes radially oriented.
- The efficient thermal conduction stabilizes this cluster until a cooling instability in the center may cause the cluster to enter a cooling core state – similar to Virgo now – and requires possibly self-regularized heating by a super-massive black hole to be stabilized.

Conclusions on magnetic draping around galaxies

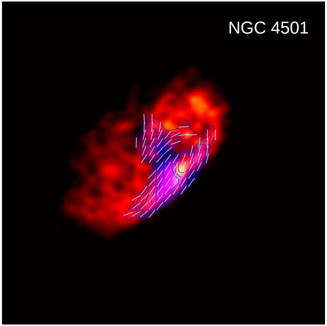

- draping of cluster magnetic fields naturally explains polarization ridges at Virgo spirals

Conclusions on magnetic draping around galaxies

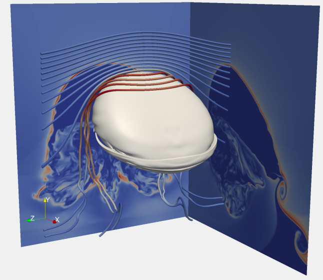

- draping of cluster magnetic fields naturally explains polarization ridges at Virgo spirals
- this represents a new tool for measuring the in situ 3D orientation and coherence scale of cluster magnetic fields

Conclusions on magnetic draping around galaxies

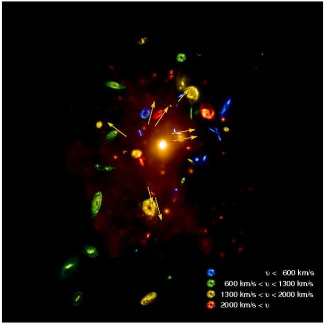

- draping of cluster magnetic fields naturally explains polarization ridges at Virgo spirals
- this represents a new tool for measuring the in situ 3D orientation and coherence scale of cluster magnetic fields
- application to the Virgo cluster shows that the magnetic field is preferentially aligned radially

Conclusions on magnetic draping around galaxies

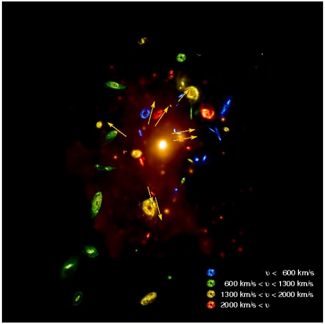

- draping of cluster magnetic fields naturally explains polarization ridges at Virgo spirals
- this represents a new tool for measuring the in situ 3D orientation and coherence scale of cluster magnetic fields
- application to the Virgo cluster shows that the magnetic field is preferentially aligned radially

- this finding implies efficient thermal conduction across clusters that stabilizes these non-cool core systems
- important implications for thermal cluster history → galaxy cluster cosmology

Literature for the talk

- Pfrommer & Jones, 2011, ApJ, 730, 22,
  Radio Galaxy NGC 1265 unveils the Accretion Shock onto the Perseus Galaxy Cluster
- Pfrommer & Dursi, 2010, Nature Phys., 6, 520,
  Detecting the orientation of magnetic fields in galaxy clusters
- Dursi & Pfrommer, 2008, ApJ, 677, 993,
  Draping of cluster magnetic fields over bullets and bubbles - morphology and dynamic effects